Dyes and Pigments 99 (2013) 299–307

Contents lists available at SciVerse ScienceDirect

Dyes and Pigments

journal homepage: www.elsevier.com/locate/dyepig

Impact of hydroxy and octyloxy substituents of phenothiazine based dyes on the photovoltaic performance

Zafar Iqbal [a,c], Wu-Qiang Wu [b], Hai Zhang [a], Peng-Li Hua [a], Xiaoming Fang [a], Dai-Bin Kuang [b,**], Lingyun Wang [a], Herbert Meier [d], Derong Cao [a,*]

[a] School of Chemistry and Chemical Engineering, State Key Laboratory of Luminescent Materials and Devices, South China University of Technology, Guangzhou 510641, China
[b] MOE Key Laboratory of Bioinorganic and Synthetic Chemistry, KLGHEI of Environment and Energy Chemistry, School of Chemistry and Chemical Engineering, Sun Yat-sen University, Guangzhou 510275, China
[c] PCSIR Laboratories Complex, Feroze pur Road, Lahore 54000, Pakistan
[d] Institute of Organic Chemistry, University of Mainz, Mainz 55099, Germany

ARTICLE INFO

Article history:
Received 20 March 2013
Received in revised form
24 May 2013
Accepted 27 May 2013
Available online 13 June 2013

Keywords:
Organic dye
Ancillary anchoring unit
Dye-sensitized solar cells
Phenothiazine
Open-circuit photovoltage
Photovoltaic performance

ABSTRACT

Two novel organic dyes containing hydroxy and octyloxy substituents onto a phenothiazine skeleton were synthesized and their effects on the photovoltaic performance were studied. Hydroxy acts as an ancillary anchoring unit along with the carboxylic group, while the phenothiazine modified moiety acts as an electron donor. The photophysical and electrochemical studies revealed that maximum absorbance of the dye with the hydroxy group in the solution was blue shifted and its band gap increased, indicating that donor acceptor strength was reduced as compared to the octyloxy substituted dye. Furthermore, electron lifetime of the organic dye with the hydroxy moiety was shorter due to smaller resistance of electron recombination. Contrarily the dye with octyloxy moiety exhibited higher electron lifetime and open-circuit photovoltage leading to an overall power conversion efficiency of 6.32% under standard AM 1.5G illumination. The IPCE was over 80% in the region between 450 and 500 nm.

1. Introduction

The increasing global demand for energy and depletion of fossil fuel reserves necessitate the development of clean alternative energy sources. Among all the renewable energy resources, solar energy is regarded as one of the most perfect energy sources that have the largest potential to cater for the future global need without appreciable greenhouse effect [1]. Solar radiation amounts to 3.8 million EJ/year, which is approximately 10,000 times more than current energy needs [2]. From the perspective of energy conservation and environmental protection, it is desirable to directly convert solar radiation into electrical power by the application of photovoltaic devices.

Dye-sensitized solar cells (DSSCs), a third generation photovoltaic technology, have attracted a great deal of interest as a promising inexpensive energy source since the first report from Grätzel in 1991 [3]. DSSCs are being considered to be a potential alternative to expensive inorganic solar cells due to low material cost, easy and inexpensive fabrication process and reasonably good power conversion efficiency [4–6]. Furthermore, dye-sensitized solar cells have been proved to perform better than conventional solar cell in some aspects, *i.e.* in the diffused light [7] and at moderate temperature – up to 50 °C [8]. Above all, DSSCs have opened up remarkable new possibilities and paradigms for producing solar photovoltaics in a green and low-cost manner.

Metals like ruthenium and zinc based dyes have been extensively studied and gave efficiencies over 10–11% [5] and 12%, respectively [6]. Ruthenium is a rare and expensive metal and its dyes have relatively low molar extinction coefficients. Furthermore, these complexes need tedious purification processes, which hamper large scale production [9]. Therefore, more efforts have been dedicated to the development of pure organic dyes, which exhibit not only higher molar extinction coefficients, but also simple preparation and purification at lower cost. In this regard, great progress has been made in this field and various electron

* Corresponding author. Tel./fax: +86 20 87110245.
** Corresponding author. Tel.: +86 20 84113015.
E-mail addresses: kuangdb@mail.sysu.edu.cn (D.-B. Kuang), drcao@scut.edu.cn (D. Cao).

0143-7208/$ – see front matter © 2013 Elsevier Ltd. All rights reserved.
http://dx.doi.org/10.1016/j.dyepig.2013.05.032

donors like triphenylamine, indoline, carbazole, merocyanine, polyene, hemicyanine, fluorene, tetrahydroquinoline, phenoxazine and phenothiazine have been explored [10–21]. However, the photovoltaic performance of metal-free organic dyes still lag behind the ruthenium complexes.

Among the components of DSSCs, the sensitizer is a crucial part, which significantly influences the power conversion efficiency as well as the stability of the device. The molecular architecture of most sensitizers includes a donor (D), a bridge (π-bridge) and an acceptor (A), which are usually combined following a D–π–A rod like configuration [22]. The efficiency of sensitization is critically dependent on electron injection from a photoexcited state of the dye into the conduction band of the semiconductor and resistance of recombination. The injection of electrons from the excited states is most likely in the vibrational mode *i.e*. hot electrons injected from the dye into the metal oxide, hence there is a mandatory requirement for proximal contact between the dye and metal oxide [23]. This suggests that the dye-metal oxide distance should be shorter and therefore the mode of linkage of dye on metal oxide needs more attention. Typically, the carboxy group has been used as an anchoring unit but it suffers hydrolysis, which inhibits the electron injection rate [24]. The carboxy group can either form an ester-like linkage (C=O) or carboxylate-like linkage (C–O–O–), resulting in the decrease of electron density of the ligand, leading to a lower energy shift in the band. Keeping in mind this factor, several groups have investigated more than one anchoring unit for efficient electron injection [25–31]. All authors have reported symmetric di-anchoring groups for efficient electron injection from the excited state of the dye to the conduction band of TiO_2 but still the efficiency lags behind. Increased carboxy groups in the dye cause decrease in electron donor-acceptor strength and also facilitate aggregation via hydrogen bonding on the surface of titanium oxide. The bottlenecks lie in either the low electron injection efficiency or the limited broadening of absorption spectra.

Hydroxy is another promising anchoring group because it can form a strong chromophores-semiconductor coupling with least spatial arrangements [32]. Hemicyanine dyes with a hydroxy group were investigated by Yao et al. [33] and Chen et al. [34] they have found that electron injection rate increases which gave better efficiency as compared to carboxy group alone. Similar study has also been reported by Huang et al., in 2009 [35]. Efficient electron injection, reduction of recombination and effective regeneration of dye are the leading factors for the enhancement of power conversion efficiency [36]. In order to absorb the sunlight as much as possible, a broad absorption spectrum of the dye is desirable. Usually, extension of π–conjugation is a feasible strategy to resolve this task. However, the large π–conjugation system leads to poor photovoltaic properties due to dye aggregation, as well as electron recombination issues. To diminish the dye aggregation and the electron recombination, the alkoxy or alkyl chains were linked to the aromatic system. Various studies have been conducted by the introduction of bulky alkoxy and aromatic rings to the donor system and improvement in the efficiencies have been observed [37–39]. Most likely, this is due to an increase in electron donation, as well as a decrease in aggregation and electron recombination reactions of the dyes on TiO_2 films.

Phenothiazine (PTZ) is a well known photosensitizer with electron-rich sulfur and nitrogen heteroatom, and its ring is non-planar with a butterfly conformation at the ground state, which can impede the molecular aggregation and the formation of molecular excimers [40]. The additional electron rich sulfur atom renders PTZ a stronger donor than other amines, even better than triphenylamine, tetrahydroquinoline, carbazole and iminodibenzyles [41,42]. PTZ based dyes containing various types of modifications have been synthesized for application in dye-sensitized solar cells [43–48].

Keeping in view the above discussion, the current concept has been developed. Two novel dyes **POH** and **POCT** through simultaneous modifications of donor and linker of PTZ were designed and synthesized for DSSCs. Dye **POH** contained hydroxy and carboxy as anchoring units with conjugate extension at the 7-position and an ethyl chain at the 10-position of PTZ, while dye **POCT** containing an octyloxyphenyl moiety at the 7-position and an ethyl chain at the 10-position of PTZ. (Scheme 1). The effects of hydroxy and octyloxy substituents on the photophysical, photochemical and photovoltaic characteristics were investigated in detail.

2. Experimental section

2.1. Instrumentation and materials

^{1}H NMR spectra were obtained on a Bruker 400 MHz spectrometer in $CDCl_3$ or DMSO-d_6 with tetramethylsilane (TMS) as the internal standard. Mass spectra (APCI–MS) were recorded on an Esquire HCT PLUS mass spectrometer. Elementary analyses were performed by using Vario EL*III* Analyzer, while melting points were taken on Tektronix X4 microscopic MP apparatus. Infrared spectra (FT–IR) were recorded on KBr pellets with Bruker Tensor 27 spectrometer. The UV–visible and fluorescent spectra of the dyes were determined in THF and CH_2Cl_2 solutions (1×10^{-5} M) and measured at room temperature by Shimadzu UV-2450 UV–Vis spectrophotometer and Fluorolog III photoluminescence spectrometer, respectively.

Electrochemical redox potentials of the dyes were measured by cyclic voltammetry (CV), using an Ingsens 1030 electrochemical work station (Ingsens Instrument Guangzhou, Co. Ltd., China) and three electrode cells in one compartment. The measurements were carried out at a scan rate of 50 mV/s. The Ag/AgCl in KCl (3 M) solution and an auxiliary platinum wire were utilized as reference and counter electrodes, while dye loaded TiO_2 films were used as a working electrode. Tetrabutylammonium perchlorate (n-Bu_4NClO_4) 0.1 M was used as supporting electrolyte in acetonitrile. All electrochemical measurements were calibrated by using ferrocene as standard (0.63 V *vs.* NHE). The photocurrent density-photovoltage characteristics were recorded by using a Keithley 2400 source meter under simulated AM 1.5 G (100 mW cm^2) illumination with a solar light simulator (Oriel, Model: 91192). A 1000 W Xenon arc lamp (Oriel, Model: 6271) served as a light source which was calibrated with an NREL standard Si solar cell. The incident photon-to-current conversion efficiency (IPCE) spectra were measured as a function of wavelength from 380 to 800 nm on the basis of a Spectral Products DK240 monochromator. The electrochemical impedance spectra (EIS) measurements were conducted on the electrochemical workstation (Zahner Zennium) in dark conditions with an applied bias potential of −0.71 V. A 10 mV AC sinusoidal signal was employed over the constant bias with the frequency ranging between 1 MHz and 10 mHz. The impedance parameters were determined by fitting the impedance spectra using Z–view software. Intensity modulated photovoltage spectroscopy (IMVS) was carried out on the electrochemical workstation (Zahner Zennium) with a frequency response analyzer under a modulated LED light (457 nm) driven by a source supply (Zahner PP211). The illumination light-intensity ranged from 30 to 150 mW cm^{-2}. The light intensity modulation was 10% or less than the base light intensity. The frequency was set in a range from 100 kHz to 0.1 Hz. The dye-loading amount was determined by desorbing the dye from the films with 0.1 M NaOH in ethanol/H_2O and measuring UV–Vis spectrum of the obtained solution [49].

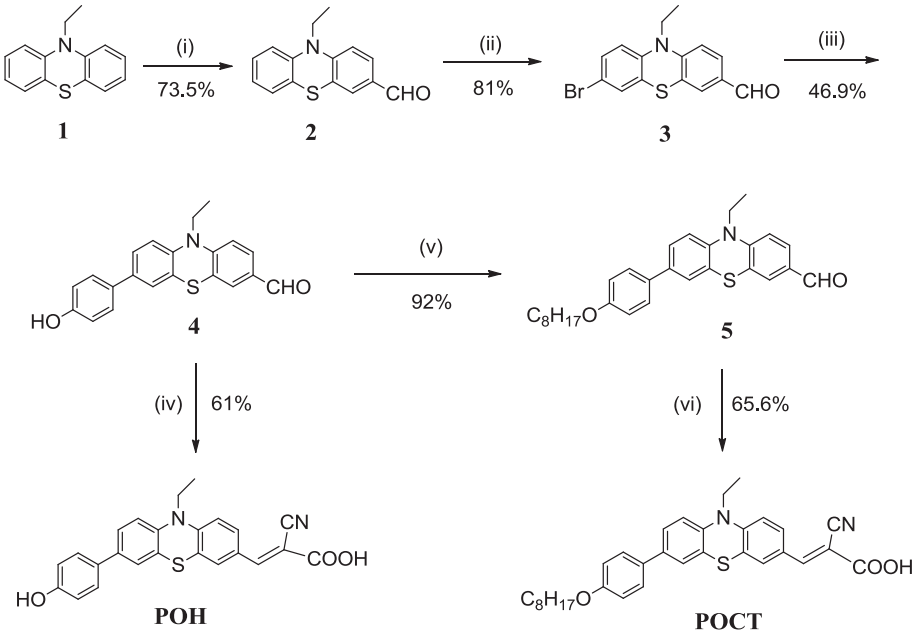

Scheme 1. Syntheses of the dyes **POH** and **POCT**. (i) DMF, $POCl_3$, 0 °C, dichloroethane, 90 °C, overnight; (ii) Chloroform, NBS, 70 °C, 6 h; (iii) 4-Hydroxyphenylboronic acid, DMF, K_2CO_3, $Pd(PPh_3)_4$, 90 °C, 36 h; (iv) Cyanoacetic acid, piperidine, acetonitrile, reflux, 7 h; (v) DMF, K_2CO_3, 1-bromooctane, 130 °C, 24 h.

10-Ethyl-10*H*-phenothiazine (**1**) was prepared from phenothiazine by alkylation in the presence of *N*,*N* dimethylformamide (DMF) followed by the synthesis of 10-ethyl-10*H*-phenothiazine-3-carbaldehyde (**2**) via Vilsmeier–Haack reactions in the presence of DMF and phosphorus oxychloride ($POCl_3$), according to reported literature [50]. The reagents including phenothiazine, *N*-bromosuccinimide (NBS), tetrakis(triphenylphosphine)palladium(0) $Pd(PPh_3)_4$, 4-hydroxyphenylboronic acid, 1-bromooctane and solvents like DMF, petroleum ether (60–90 °C, PE), dichloromethane (DCM), tetrahydrofuran (THF) and chloroform were purchased as reagent grade and used without purification. All reactions were performed under nitrogen or argon and monitored by TLC (Merck 60 F254) and purified by column chromatography on silica gel (200–300 mesh).

2.2. Synthesis of dyes

2.2.1. 10-Ethyl-10H-phenothiazine-3-carbaldehyde (2)

$POCl_3$ (6.90 g, 45 mmol) was added drop wise to the freshly distilled *N*,*N*-dimethylformamide (3.29 g, 45 mmol) at 0 °C under a nitrogen atmosphere. Stirring was continued until a solid glassy material appeared which was dissolved in dichloroethane (50 mL) and stirred for an additional 1 h. Then compound **1** (2.05 g, 9 mmol) dissolved in dichloroethane (15 mL) was injected into the flask and maintained at 90 °C overnight. When the reaction was finished (TLC monitoring), the reaction mixture was cooled to room temperature and poured into water. The obtained mixture was neutralized with dilute solution of NaOH. The product was extracted with dichloromethane (250 mL). The organic layer was separated, washed with water and dried over anhydrous Na_2SO_4. The solvent was removed under reduced pressure and the crude product was purified by column chromatography using silica gel and petroleum ether/dichloromethane (PE/DCM, 1:1) as the mobile phase to obtain the required product **2** as a yellow solid (1.69 g) in 73.5% yield, mp 82–84 °C. ^1H NMR ($CDCl_3$, 400 MHz, ppm): δ 9.75 (s, 1H), 7.60–7.58 (m, 1H), 7.53–7.52 (m, 1H), 7.15–7.11 (m, 1H), 7.07–7.05 (m, 1H) 6.95–6.91 (m, 1H), 6.87–6.85 (m, 2H), 3.95–3.90 (m, 2H), 1.41 (t, J = 6.8 Hz, 3H).

2.2.2. 7-Bromo-10-ethyl-10H-phenothiazine-3-carbaldehyde (3)

10-Ethyl-10*H*-phenothiazine-3-carbaldehyde **2** (1.28 g, 5.0 mmol) was dissolved in $CHCl_3$ (25 mL) at 0 °C and maintained for half an hour. Then *N*-bromosuccinimide (NBS) (1.06 g, 6.0 mmol) dissolved in chloroform (10 mL) was injected slowly under nitrogen and the temperature raised to 70 °C. The reaction was completed in 6 h. After cooling, the reaction mixture was poured into the water and extracted with CH_2Cl_2 (250 mL). The organic layer was separated and washed three times with brine solution. Then it was dried over anhydrous Na_2SO_4 and solvent was removed under reduced pressure. The desired product was purified by column chromatography, using silica gel and PE/DCM (1:1) as the mobile phase to obtain the required product **3** as a yellow solid (1.36 g) in 81% yield, mp 99–101 °C. ^1H NMR ($CDCl_3$, 400 MHz, ppm): δ 9.80 (s, 1H), 7.65–7.63 (m, 1H), 7.56–7.55 (m, 1H), 7.26–7.23 (m, 1H), 7.21–7.20 (m, 1H) 6.91–6.89 (m, 1H), 6.74–6.71 (m, 1H), 3.96–3.91 (m, 2H), 1.43 (t, J = 6.8 Hz, 3H).

2.2.3. 10-Ethyl-7-(4-hydroxyphenyl)-10H-phenothiazine-3-carbaldehyde (4)

A mixture of the 7-bromo-10-ethyl-10*H*-phenothiazine-3-carbaldehyde **3** (1.34 g, 4 mmol), DMF (20 mL), aqueous solution of K_2CO_3 (2 M, 10 mL) and $Pd(PPh_3)_4$ (10 mol %) was heated to 40 °C for half an hour under argon. Then 4-hydroxyphenylboronic acid (0.64 g, 4.5 mmol) dissolved in DMF (10 mL) was injected slowly into the reaction mixture. The temperature of the reaction mixture was raised to 90 °C and maintained for 36 h. After cooling, it was dropped into water (500 mL) and extracted with CH_2Cl_2 (150 mL). The organic layer was washed several times with water (250 mL each), then dried over anhydrous Na_2SO_4. The solvent was evaporated under reduced pressure and purification was carried out by column chromatography using silica gel and DCM as the mobile phase to give compound **4** as an orange color solid (0.57 g) in 46.9% yield, mp 183–184 °C. ^1H NMR ($CDCl_3$, 400 MHz, ppm): δ 9.81 (s, 1H), 7.67–7.65 (m, 1H), 7.61–7.60 (m, 1H), 7.44–7.41 (m, 2H), 7.35–7.32 (m, 1H) 7.29–7.28 (m, 2H), 6.95–6.90 (m, 3H), 4.04–3.99 (m, 2H), 1.50 (t, J = 6.8 Hz, 3H). FT–IR (KBr pellet, cm^{-1}): 3400, 3055, 2926, 2854, 1667, 1580, 1568, 1507, 1289, 1248. APCI–MS: *m/z* 347.10. Found:

347.90 $[M + H]^+$. Anal. Calcd. for $C_{21}H_{17}NO_2S$: C, 72.60; H, 4.93; N, 4.03; S, 9.23; found: C, 72.85; H, 4.92; N, 4.23; S, 9.19.

2.2.4. 10-Ethyl-7-(4-(octyloxy)phenyl)-10H-phenothiazine-3-carbaldehyde (**5**)

A mixture of compound **4** (0.26 g, 0.75 mmol), K_2CO_3 (0.31 g, 2.25 mmol) and DMF (30 mL) was stirred for half an hour at room temperature and then 1-bromooctane (0.29 g, 1.5 mmol) was injected under nitrogen. Temperature was raised to 130 °C and maintained for 24 h. After cooling, the reaction mixture was poured into water (500 mL) and stirred for half an hour. Then CH_2Cl_2 (250 mL) was added and the organic layer was separated. The organic layer was washed several times with water, dried over anhydrous Na_2SO_4 and solvent was removed by rotary evaporator. The crude product was purified by column chromatography using silica and PE/DCM (1:1) as the mobile phase to yield compound **5** (0.32 g, 92%), a bright yellow solid, mp 92–93 °C. ^{1}H NMR ($CDCl_3$, 400 MHz, ppm): δ 9.80 (s, 1H), 7.66–7.63 (m, 1H), 7.59–7.58 (m, 1H), 7.47–7.45 (m. 2H), 7.36–7.33 (m, 1H), 7.30–7.28 (m, 1H), 6.98–6.95 (m, 2H), 6.94–6.90 (m, 2H), 4.02–3.97 (m, 4H), 1.86–1.79 (m, 2H), 1.50–1.47 (m, 5H), 1.38–1.29 (m, 8H), 0.92 (t, $J = 6.4$ Hz, 3H). FT–IR (KBr pellet, cm^{-1}): 3062, 2925, 2854, 1678, 1607, 1580, 1505, 1296, 1245. APCI–MS: *m/z* 459.20. Found: 460.20 $[M + H]^+$. Anal. Calcd. for $C_{29}H_{33}NO_2S$: C, 75.78; H, 7.24; N, 3.05; S, 6.98; found: C, 75.82; H, 7.34; N, 3.27; S, 6.79.

2.2.5. 2-Cyano-3-(10-ethyl-7-(4-hydroxyphenyl)-10H-phenothiazin-3-yl)acrylic acid (***POH***)

A mixture of compound **4** (0.21 g, 0.6 mmol), cyanoacetic acid (0.51 g, 6.0 mmol), piperidine (0.3 mL, 3 mmol) in acetonitrile (35 mL) was refluxed for 7 h under nitrogen. After cooling, the mixture was poured into aqueous solution of HCl (2 M, 100 mL). It was stirred for 15 min and CH_2Cl_2 (200 mL) was added. The organic layer was separated and washed again two times with water (200 mL). Then the organic layer was dried over anhydrous Na_2SO_4. The solvent was removed under reduced pressure and the crude product was purified by column chromatography using silica gel. First, it was eluted with DCM and then by DCM/CH_3OH (20:1) to yield compound **POH** (0.15 g, 61%) as reddish black solid, mp 222–223 °C. ^{1}H NMR (DMSO-d_6, 400 MHz, ppm): δ 7.88 (s, 1H), 7.75–7.70 (m, 2H), 7.46–7.39 (m, 3H), 7.35–7.34 (m, 1H), 7.09–7.04 (m, 2H), 6.88–6.87 (m, 2H), 3.99–3.93 (m, 2H), 1.33 (t, $J = 6.3$, 3H). FT–IR (KBr pellet, cm^{-1}): 3445, 3067, 2925, 2853, 2215, 1620, 1589, 1510, 1284, 1248. APCI–MS: *m/z* 414.10. Found: 414.90 $[M + H]^+$. Anal. Calcd. for $C_{24}H_{18}N_2O_3S$: C, 69.55; H, 4.38; N, 6.76; S, 7.74; found: C, 69.65; H, 4.70; N, 6.86; S, 7.56.

2.2.6. 2-Cyano-3-(10-ethyl-7-(4-(octyloxy)phenyl)-10H-phenothiazin-3-yl)acrylic acid (***POCT***)

Prepared by the same synthetic procedure as for compound **POH**. Compound **5** was used instead of compound **4** to give compound **POCT** as dark black solid in 65.6% yield, mp 158–159 °C. ^{1}H NMR (DMSO-d_6, 400 MHz, ppm): δ 8.03 (s, *br*, 1H), 7.87–7.85 (m, 1H), 7.79–7.78 (m, 1H), 7.59–7.56 (m, 2H), 7.47–7.45 (m, 1H), 7.41–7.40 (m, 1H), 7.16–7.10 (m, 2H), 7.00–6.98 (m, 2H), 4.03–3.98 (m, 4H), 1.77–1.70 (m, 2H), 1.45–1.41 (m, 2H), 1.37 (t, $J = 6.4$ Hz, 3H), 1.31–1.25 (m, 8H), 0.89 (t, $J = 6.8$ Hz, 3H). FT–IR (KBr pellet, cm^{-1}): 3444, 3061, 2926, 2854, 2216, 1618, 1589, 1510, 1291, 1247. APCI–MS: *m/z*, 526.23. Found: 527.20 $[M + H]^+$. Anal. Calcd. for $C_{32}H_{34}N_2O_3S$: C, 72.97; H, 6.51; N, 5.32; S, 6.09; found: C, 72.92; H, 6.67; N, 5.37; S, 6.07.

2.3. Fabrication of the dye-sensitized solar cells

Optically transparent fluorine-doped tin oxide (FTO) conducting glasses (Nippon SheetGlass, Japan) were cleaned with detergent, water, ethanol and acetone in an ultrasonic bath for removing unwanted materials. Anatase TiO_2 nanoparticles (20 nm) were prepared through a hydrothermal treatment with a precursor solution containing $Ti(OBu)_4$ (10 mL), ethanol (20 mL), acetic acid (18 mL) and deionized water (50 mL) according to the previously reported paper [51]. The prepared TiO_2 powder (1.0 g) was ground for 40 min in a mixture of ethanol (8.0 mL), acetic acid (0.2 mL), terpineol (3.0 g) and ethyl cellulose (0.5 g). After that, homogenized slurry was sonicated for 15 min in an ultrasonic bath to form a viscous white TiO_2 paste. Then the paste was screen-printed onto FTO glass and TiO_2 photoanodes (about 16 μm in thickness) were prepared. Annealations of the prepared films were performed through a procedure (325 °C for 5 min, 375 °C for 5 min, 450 °C for 15 min, and 500 °C for 15 min) in a muffle furnace to remove the organic substances. TiO_2 films were soaked in $TiCl_4$ (0.04 M) aqueous solution for 30 min at 70 °C for the improvement of photocurrent and photovoltaic performance. Then treated films were rinsed with deionized water and ethanol and sintered again at 520 °C for 30 min. After cooling to 80 °C, the films were immersed in a 5.0×10^{-4} M solution of **POH** and **POCT** dyes for 16 h (dyes solution in a mixture of tetrahydrofuran and dichloromethane, 1:1 volume ratio). Films were taken out of solution and rinsed with CH_2Cl_2 in order to remove physical adsorbed organic dye molecules. The dye-sensitized TiO_2/FTO glass films were assembled into a sandwiched type together with Pt/FTO counter electrode to evaluate their photovoltaic performance. Platinized counter electrodes were fabricated by thermal depositing of H_2PtCl_6 (5 mM in isopropanol) solution onto FTO glass followed by heating at 400 °C for

Table 1
Absorption and emission characteristics of the dyes **POH** and **POCT**.

Dye	Absorption λ_{max} (nm) [a]	ε (M^{-1} cm^{-1})[b]	Emission λ_{max} (nm)[c]	Absorption λ_{max} (nm)[d]	Blue shift of λ_{max} (nm)[e]
POH	299, 446	53250, 18800	572	427	19
POCT	304, 460	37900, 16100	611	454	6

[a] Absorption maximum of dyes measured in THF/DCM (1:1) with concentration 1×10^{-5} mol/L.
[b] The molar extinction coefficient at λ_{max} in solution.
[c] Emission maximum of dyes in THF/DCM (1:1) with concentration 1×10^{-5} mol/L.
[d] Absorption maximum of dyes adsorbed on the surface of TiO_2.
[e] Absorption λ_{max}.

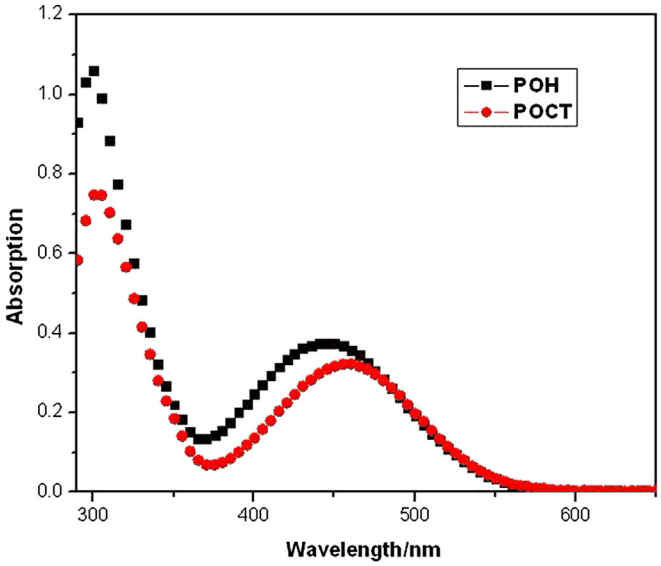

Fig. 1. Normalized absorption spectra of the dyes **POH** and **POCT**.

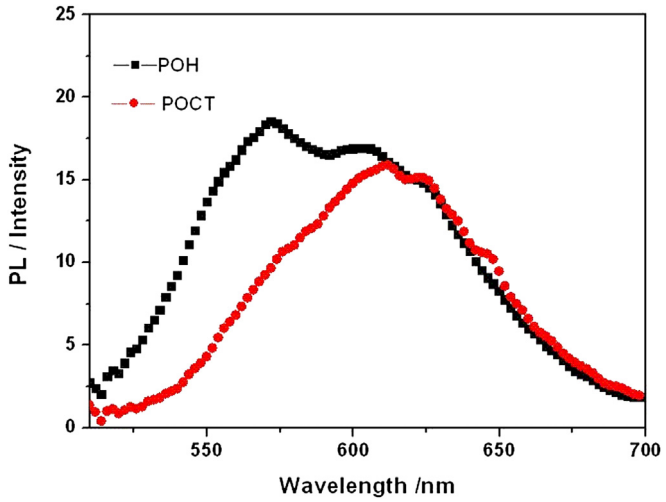

Fig. 2. Normalized emission spectra of the dyes **POH** and **POCT**.

15 min in air. The electrolyte (0.6 M 1-methyl-3-propylimidazolium iodide (PMII), 0.10 M guanidinium thiocyanate, 0.05 M LiI, 0.03 M I_2 and 0.5 M tert-butylpyridine) in acetonitrile/valeronitrile (85:15) was injected from a hole made on the counter electrode into the interspace between the photoanode and counter electrode. The active area of the dye coated TiO_2 film was 0.16 cm^2 and aperture size of black mask used was about 0.25 cm^2.

3. Results and discussion

3.1. Synthesis and structural characterization

The synthetic route of the dyes is shown in Scheme 1. Phenothiazine was purchased while 10-ethyl-10H-phenothiazine (**1**) was prepared by the alkylation reaction with ethyl bromide in the presence of DMF. Formylation of compounds **1** was carried out by the Vilsmeier–Haack reactions in the presence of DMF and $POCl_3$ to give compound **2**. This reagent was brominated with NBS in chloroform to give compound **3**. Suzuki coupling reaction of compound **3** was carried out with 4-hydroxyphenylboronic acid to give compound **4**, which was alkylated in the presence of DMF and potassium carbonate to give compound **5**. Finally, the compound **4** was converted to the dye **POH**, while compound **5** was converted to dye **POCT** by the Knoevenagel condensation reaction. All the intermediates and targeted dyes were confirmed by standard spectroscopic methods.

3.2. Photophysical properties

UV–Vis absorption and emission spectra of the dyes **POH** and **POCT** in THF/DCM (1:1) solution (1×10^{-5} M) and adsorbed on a thin TiO_2 film are presented in Table 1, Figs. 1 and 2. The UV spectra of the dyes exhibited two distinct bands, one at 299, 304 nm and the other at 446, 460 nm. The first band corresponds to the $\pi-\pi^*$ transition of the localized conjugated skeleton in the UV region, while the second band was assigned to an intramolecular charge transfer (ICT) in the visible region. UV absorption λ_{max} increases by 14 nm from **POH** with hydroxy group to **POCT** with octyloxy group, which imparts a strong electron donating capability. The blue shift of dye **POH** with hydroxy unit was attributed to its decreased donor and acceptor strength [52]. Molar extinction coefficients (ε) of the dyes **POH** and **POCT** were 18800 M^{-1} cm^{-1} and 16100 M^{-1} cm^{-1}, respectively. The higher value of ε for dye **POH** was due to the larger oscillator strength of the charge transition, according to Frank-Condon principle [26,53]. After being adsorbed on the surface of TiO_2 films, λ_{max} of both dyes **POH** and **POCT** was blue shifted to 19 nm and 6 nm as compared to the solution (Table 1). It appears to be a common phenomenon for organic dyes, which has been ascribed to the deprotonation of anchoring groups as well as to the formation of aggregation on the semiconductor surface [54].

Dye load amounts of the dyes **POH** and **POCT** were 1.56×10^{-7} mol cm^{-2} and 1.63×10^{-7} mol cm^{-2}, respectively (Table 3). The dye **POH** has lower dye load amount owing to the presence of hydroxy unit which might increase the contact area between dye molecule and TiO_2, which subsequently leads to a decreased adsorption of the dye per unit surface area of TiO_2 film [33,34].

The dye **POH** has hydroxy and carboxy as anchoring groups whereas the dye **POCT** has only a carboxy group. Their mode of attachments were studied by fourier transform infrared spectrtoscopy (FT-IR). Characteristic bands for –C≡N were observed at 2219 cm^{-1} and 2211 cm^{-1} while the –C=O stretching bands of the carboxyl groups were observed at 1693 cm^{-1} and 1697 cm^{-1} for **POH** and **POCT** dyes, respectively. Upon dye adsorption to the TiO_2 surface, –C=O stretching bands at 1693 cm^{-1} and 1697 cm^{-1} disappeared and new asymmetric stretching bands at 1607 cm^{-1} and 1626 cm^{-1} and symmetric stretching bands at 1382 cm^{-1} and 1383 cm^{-1} for carboxylate units appeared in the spectra of **POH** and **POCT** dyes [28,55,56]. Additionally, compared to **POCT** dye an intense band at 1116 cm^{-1} for **POH** dye spectra was observed, which was due to –C–O– stretching. This observation indicates that the hydroxy group was also involved in anchoring with the TiO_2 surface, similar findings have also been reported [25,57].

Table 3
Photovoltaic parameters of DSSCs based on dyes **POH** and **POCT**.

Dyes	CDCA	J_{SC} (mA/cm^{-2})	V_{oc} (mV)	FF	η (%)	Electron lifetime (τ_r, ms)	R_2 (ohm)	Dye load amount (mol cm^{-2})
POH	0	11.28	677	0.69	5.23	64.0	51.6	1.56×10^{-7}
	1 mmol	8.54	779	0.75	4.96	– [a]	– [a]	– [a]
POCT	0	12.47	741	0.68	6.32	110	102.2	1.63×10^{-7}
	1 mmol	11.18	787	0.70	6.19	– [a]	– [a]	– [a]

[a] Unmeasured.

Table 2
Electrochemical characteristics of the dyes **POH** and **POCT**.

Dyes	λ(nm)[a]	HOMO (V) *vs.* NHE[b]	E_{0-0} (eV) *vs.* NHE[c]	LUMO (V) *vs.* NHE[d]	HOMO (eV) *vs.* Vacuum[e]	LUMO (eV) *vs.* Vacuum[e]	E-gap (eV)
POH	494.4	1.35	2.39	−1.04	−5.39	−2.89	−2.50
POCT	508.2	1.47	2.29	−0.82	−5.33	−2.91	−2.42

[a] λ intersection obtained from the cross point of absorption and emission spectra in THF/DCM (1:1) solution.
[b] HOMO of dyes measured by cyclic voltametery in 0.1 M tetrabutylammonium perchlorate in acetonitrile solution as supporting electrolyte, Ag/AgCl as reference electrode and Pt as counter electrode.
[c] $E_{0-0} = 1240/\lambda$ intersection.
[d] LUMO was estimated by HOMO–E_{0-0}.
[e] HOMO and LUMO were calculated at B3LYP-3 G(d, p) level in vacuum.

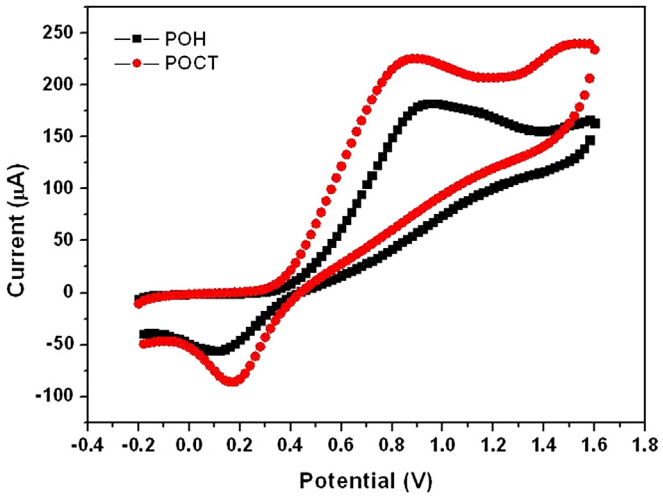

Fig. 3. Cyclic voltammetry of the dyes **POH** and **POCT**.

3.3. Electrochemical properties

In order to investigate the possibilities of electron transfer from the excited states of **POH** and **POCT** dyes to the conduction band of TiO_2 and regeneration of the dyes, the redox behavior was studied by cyclic voltammetry (Fig. 3, Table 2). The first oxidation potentials of the dyes enabled the calculation of the highest occupied molecular orbitals (HOMO) of 1.35 V and 1.47 V (*vs*. NHE) for **POH** and **POCT**, respectively. The lowest unoccupied molecular orbitals (LUMO) were estimated by oxidation potential and the energy at the intersection of absorption and emission spectra, which were − 1.04 V and − 0.82 V for **POH** and **POCT**, respectively. The band gap of **POH** was higher than **POCT**, which may be due to two anchoring units i.e hydroxy and carboxy. Introduction of more anchoring groups results in an increased variation of molecular orbitals energies. Furthermore, increased anchoring unit numbers decrease the donor and acceptor strength [52]. Furthermore, the LUMO level of **POH** was higher than the dye **POCT** indicating that it has more driving force for electron injection as compared to the dye **POCT**. Contrarily, HOMO level of the dye **POH** was less positive than the dye **POCT**, indicating that its regeneration capacity of the oxidized dye will be affected. Overall, both LUMO levels and HOMO levels of the dyes **POH** and **POCT** are reasonably suitable for providing sufficient thermodynamics driving force for electron injection from the excited state to the conduction band of TiO_2 (0.5 eV *vs*. NHE) [58] and regeneration from I^-/I_3^- redox potential (0.4 eV *vs*. NHE) [59]. The requirement for appropriate electron injection from the excited state to the conduction band of titanium dioxide is 0.2 eV [60].

3.4. Molecular orbital calculations

To gain further insight into the above mentioned results, density function theory (DFT) calculations were carried out by using Gaussian 09 software at the B3LYP/6-31G (d, p) levels [61]. Optimized structures and the electronic distribution in HOMO and LUMO levels are presented in Fig. 4, Table 2. The electron distributions of the **POH** and **POCT** in the HOMOs levels were mainly localized on the phenothiazine moiety, while the LUMOs showed localized electron distribution through the cyanoacrylic acid upon light illumination. Therefore, HOMO–LUMO excitation by light, induced shift of the electron from the PTZ donor moiety to the acceptor moiety. This separation of electrons ensures the efficient electron injection from the dye to the TiO_2 film. The octyloxy chain attatched at the 7-position and ethyl chain on the N atom of PTZ may increase the bulkiness of the molecule, which prevents the formation of excimers and aggregates on the TiO_2 surface [62].

3.5. Photovoltaic performance of the DSSCs

In order to investigate the photovoltaic performance of the dyes, a set of dye-sensitized solar cells was fabricated as described in the experimental section and tested under standard conditions (AM 1.5 G, 100 mW cm^{-2}). The incident photon-to-current efficiency (IPCE) and photocurrent density–photovoltage (*J*–*V*) curves of the dyes **POH** and **POCT** were obtained with a sandwich cell comprising of 16 μm TiO_2 photoanode and I^-/I_3^- redox electrolyte.

The IPCE spectra of **POH** and **POCT** for DSSCs are plotted as a function of wavelength from 380 nm to 800 nm as seen in Fig.6. The maximum IPCE values for the dyes **POH** and **POCT** were attained at 480 nm and 450 nm, respectively. The dye **POH** reached over 70% in the range of 390 nm–540 nm with tail off at 670 nm while dye **POCT** reached over 70% in the range of 380 nm–550 nm with tail off at 700 nm. Interestingly, the IPCE values reached over 80% in the region between 450 and 500 nm. Dye **POCT** has a little higher IPCE value than **POH** due to its broader absorption spectra and better light-harvesting efficiency in the visible region. This trend of IPCE spectra (**POCT** > **POH**) is in good accordance with J_{sc} data obtained in *J*–*V* measurements, indicating that dyes with higher wavelength

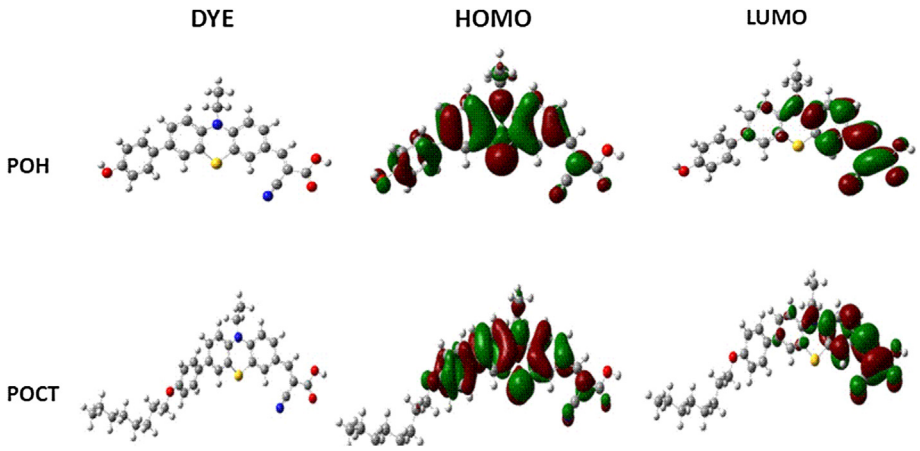

Fig. 4. Optimized structures and frontier molecular orbitals HOMO and LUMO calculated by DFT on a B3LYP/6-31+G (d, p) level.

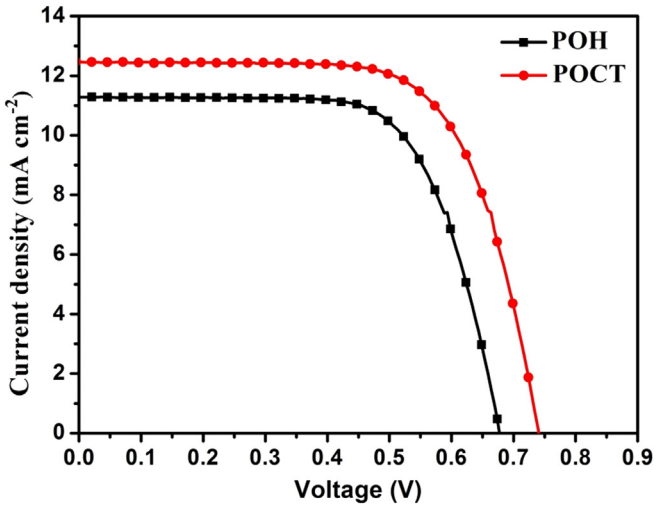

Fig. 5. *J–V* curves of DSSCs sensitized by the dyes **POH** and **POCT**.

absorption have higher J_{sc} [29]. The IPCE over 80% in the range between 420 and 580 nm with phenoxazine based dye has been reported due to intense absorption and effective intramolecular energy transfer process [63]. IPCE extended over whole visible range was obtained by Sun et al., in 2009 due to better light harvesting capability of the dye [64].

The detailed parameters of short-circuit photocurrent density (J_{sc}), open-circuit photovoltage (V_{oc}), fill factor (FF) and overall conversion efficiency (η) were obtained from photocurrent density–photovoltage curves and are summarized (Fig. 5 and Table 3). The cell based on dye **POCT** exhibits a maximum power conversion efficiency (η) of 6.32% (J_{sc} = 12.47 mA cm^{-2}, V_{oc} = 741 mV, FF = 0.68), under standard global AM 1.5G one sun illumination (100 mW cm^{-2}). Under similar measuring conditions, dye **POH** showed J_{sc} of 11.28 mA cm^{-2}, V_{oc} of 677 mV and FF of 0.69 corresponding to η of 5.23%. UV absorption maxima in solution and CV studies revealed that dye **POCT** has better electron donor-acceptor strength as compared to dye **POH**, which influence the overall power conversion efficiencies. Furthermore, Su et al. have reported that alkoxy chain is able to reduce aggregation [38] while Huang et al. have reported that the dye with hydroxyl group suffers more aggregation on the surface of TiO_2 [35]. The dye **POCT** has better short-circuit photocurrent density as compared to the dye **POH** due to the extended conjugation [63]. Furthermore, the dye loading amount of the dye **POCT** was higher than that of the dye **POH**, which is also a reason for higher value of J_{sc} for the fommer [65].

After being adsorbed on the surface of TiO_2, both dyes **POH** and **POCT** were 19 nm and 6 nm blue shifted, indicating that both dyes form aggregations. When **POH** and **POCT** were tested with CDCA (1 mmol), the J_{sc} of 8.54 mA cm^{-2} and 11.18 mA cm^{-2}, V_{oc} of 779 mV and 787 mV, FF of 0.75 and 0.70, corresponding to efficiencies of 4.96% and 6.19% were obtained, respectively (Table 3). The coadsorption of CDCA would decrease the amount of adsorbed dye on the TiO_2 surface, leading to decrease of J_{sc} [66]. However, CDCA would suppress the aggregation of the dyes, which is beneficial to increase V_{oc} and FF [67].

J–V results indicate that the V_{oc} values of **POH** are lower than **POCT.** To illustrate the difference in V_{oc} between the DSSCs based on these two dyes and investigate the interfacial charge transfer process within DSSCs, the electrochemical impedance spectra (EIS) was performed in the dark condition under a forward bias of −0.71 V. As shown in Fig. 7, two semicircles were observed in each Nyquist plot. The smaller (higher frequency from 10^3–10^6 Hz) and larger semicircles (lower frequency from 1–10^3 Hz) in the Nyquist plots were attributed to the charge transfer at the counter electrode/electrolyte interface and the TiO_2/dye/electrolyte interface, respectively. Specifically, small circles were almost similar in both dyes based DSSCs due to the use of the same counter electrode and electrolyte. On the other hand, there was a substantial difference in the large semicircles, which indicates that charge transfer behavior between TiO_2 and dye or between dye and electrolyte was significantly altered, which was likely due to the surface modifications with different dyes. The R_2 value (electron recombination resistance) obtained by fitting the large semicircles in the plots shows that **POCT** has a larger electron recombination resistance than **POH** [68], indicating **POH** is easy to suffer electron recombination. The dye **POCT** has octyloxy substituent which may form a compact structure and its hydrophobic capability reduces the recombination rates. Furthermore, octyloxy chain also plays an important role to reduce aggregation on the TiO_2 surface. The

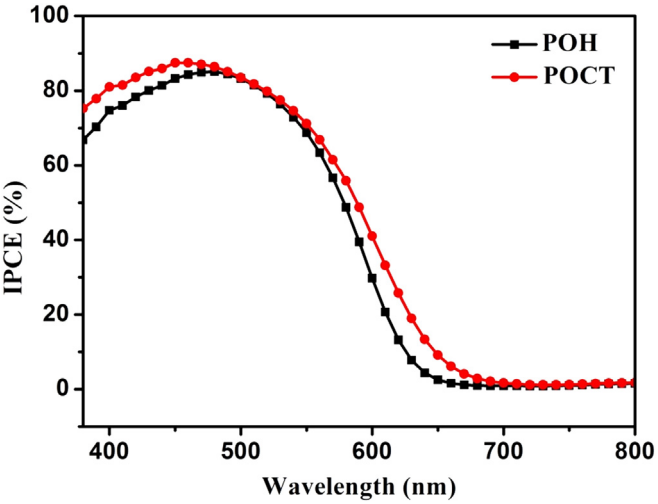

Fig. 6. IPCE spectra of DSSCs based on the dyes **POH** and **POCT**.

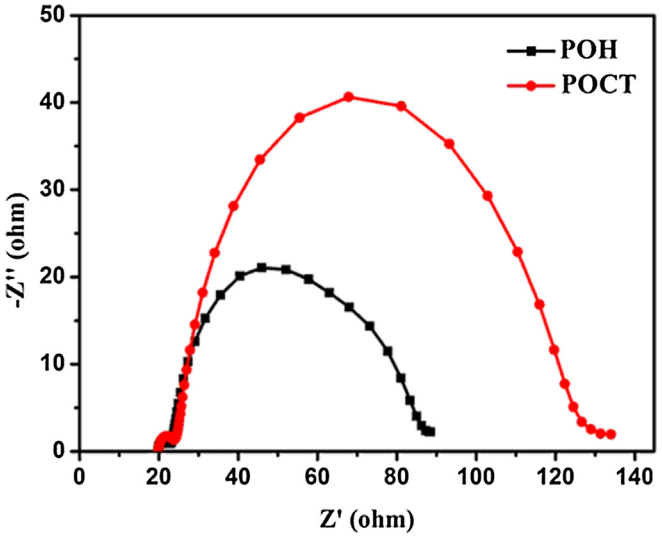

Fig. 7. Electrochemical impedance spectra of the dyes **POH** and **POCT** measured in the dark condition.

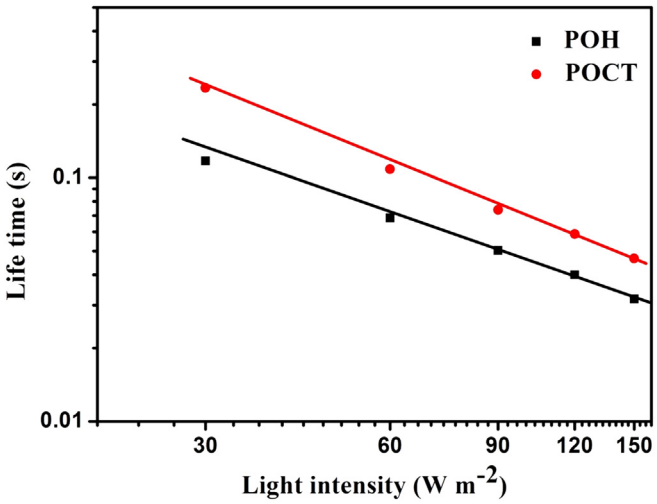

Fig. 8. IMVS spectra of the DSCCs based on dyes **POH** and **POCT** measured under various incident light intensities.

electron lifetime (τ_r) values calculated by fitting the equation $\tau_r = R_{rec} \times CPE2$ (CPE2, chemical capacitance) [69] were 64 and 110 ms for **POH** and **POCT** sensitized solar cells, respectively. Here, the longer electron lifetime of **POCT** compared to **POH**-sensitized solar cell is associated with more effective suppression of the back reaction of the injected electron with the I_3^- in the electrolyte, and thus leading to increase in V_{oc} [63]. Similar studies have been reported and demonstrated that octyloxy chain plays an important role in prolonging the electron lifetime [39,70]. These results are in good agreement with the variation tendency of V_{oc} (**POCT > POH**) measured by the *J–V* curves. To study the internal dynamics of the cells, intensity modulated phtovolatage spectroscopy (IMVS) was measured under an illumination of a LED light source ($\lambda = 457$ nm) with different light intensities from 30 to 150 W m^{-2} as denoted in Fig. 8. Clearly, electron lifetime of **POCT** was longer than **POH** based DSSCs. It is inferred that dye **POCT** has better capability of protecting the injected electron from the recombination process rendering the higher V_{oc}. These results are well in agreement with the cell performances. As the dye **POH** has two anchoring units which upon adsorption transfer more protons to the TiO_2 surface, leading to the positive shift of the conduction band edge of TiO_2. This positive shift of the conduction band reduces the gap between the fermi level of TiO_2 and redox potential of elelctrolyte, leading to decrease of open-circuit voltage [26,31].

It is emphatic to describe that factors such as orientation, nature of binding and structure of the dyes could influence the photovoltaic parameters and thereby affect the performance of DSSC. In the present work, we have found that the octyloxy chain perform better than hydroxyl unit due to its better electron donating capacity and suppression of recombination.

4. Conclusions

Two novel dyes (**POH** and **POCT**) based on modifications of phenothiazine with hydroxy and octyloxy substituents were designed and synthesized. The effect of substituents on the performance of DSSCs based on **POH** and **POCT** dyes were studied. The dye **POCT** with octyloxy unit was found superior to the dye **POH** with hydroxyl unit due to better electron donation, suppression of recombination. Under standard global AM 1.5G one sun illumination, the dye **POCT** with octyloxy unit displayed the best results with J_{sc} of 12.47 mA cm^{-2}, V_{oc} of 741 mV and FF of 0.68, corresponding to an overall power conversion efficiency of 6.32%. Under similar measuring conditions, the dye **POH** sensitized cell gave a J_{sc} 11.28 mA cm^{-2}, an V_{oc} of 677 mV and an FF of 0.69, corresponding to an overall power conversion of 5.23%. The IPCE of both the dyes reached over 80% in the region between 450 and 500 nm. The EIS results were in good agreement with the results of open-circuit photovoltages of the DSSCs based on **POH** and **POCT**. Our work demonstrate that introduction of octyloxy substituent on PTZ could improve photovoltaic performance as compared to hydroxy substituent. As the spectral response of **POCT** was not enough, further work to extend the spectral response of the dye is in progress. It is expected that, by designing a balanced molecular structure, higher efficiency could be achieved.

Acknowledgment

We are grateful to the National Natural Science Foundation of China (21272079, 20873183 and 21072064), the Natural Science Foundation of Guangdong Province, China (10351064101000000 and S2012010010634) and the Fund from Guangzhou Science and Technology Project, China (2012J4100003) for the financial support.

References

[1] Razykov TM, ferekides CS, Morel D, Stefankos E, Ullal HS, Upadhaya HM. Solar photovoltaic electricity: current status and future prospects. Sol Energy 2011;85:1580–608.
[2] Husan MA, Sumathy K. Photovoltaic thermal module concepts and their performance analysis: a review. Renew Sustain Energy Rev 2012;16:5848–60.
[3] O'Regan B, Grätzel M. A low-cost high efficiency solar cell based on dye sensitized colloidal titanium dioxide films. Nature 1991;353:737–40.
[4] Ito S, Miura H, Uchida S, Takata M, Sumiok K, Liska P, et al. High conversion-efficiency organic dye-sensitized solar cells with a novel indoline dye. Chem Commun 2008:5194–6.
[5] Chiba Y, Islam A, Watanabe Y, Komiya R, koide N, Han L. Dye sensitized solar cells with conversion efficiency of 11.1%. Jpn J Appl Phys 2006;45:L638–40.
[6] Yella A, Lee HW, Tsao HN, Yi C, Chandiran Ak, Nazeerudin MK, et al. Porphyrin-sensitzed solar cells with cobalt(II/III)-based redox electrolyte exceed 12 percent efficiency. Science 2011;334:629–34.
[7] Toyoda T, Sano T, Nakajima J, Doi S, Fukumoro S, Ito A, et al. Outdoor performance of large scale DSC modules. J Photochem Photobiol 2004;164:203–7.
[8] Berginc M, Opara KM, Jankovec M, Topie M. The effect of temperature on the performance of dye sensitized solar cells based on propyl-methyl-imidazolium idodide electrolyte. Sol Energy Mater Sol Cells 2007;91:821–8.
[9] Mishra A, Fischer MKR, Bauerle P. Metal-free organic dyes for dye sensitizedsolar cells: from structure: property relationship to design rules. Angew Chem Int Ed 2009;48:2474–99.
[10] Cheng HM, Hsieh WF. Electron transfer properties of organic dye sensitized solar cells based on indoline sensitizer with ZnO nanoparticles. Nanotech 2010;21:485202–10.
[11] Wang ZS, Koumura N, Cui Y, Takahashi M, Sekiguchi H, Mori A, et al. Hexylthiophene-functionalized carbazole dyes for efficient molecular photovoltaic: tuning of solar-cell performance by structural modification. Chem Mater 2008;20:3993–4003.
[12] Ono T, Yamaguchi T, Arakawa H. Study on dye sensitized solar cell using novel infrared dye. Sol Energy Mater Sol Cells 2009;93:831–5.
[13] Hara K, Sao T, Katoh R, Furube A, Yoshihara T, Murai M, et al. Novel conjugated organic dyes for efficient dye-sensitized solar cells. Adv Funct Mater 2005;15:246–52.
[14] Chen Z, Li F, Huang C. Organic D-π-A dyes for dye sensitized solar cells. Curr Org Chem 2007;11:1241–58.
[15] Kim S, Lee JK, Kang SO, Ko J, Yum JH, Fantacci S, et al. Molecular engineering of organic sensitizers for solar cell applications. J Am Chem Soc 2006;128:16701–7.
[16] Chen R, Yang X, Tian H, Wang X, Hagfeldt A, Sun L. Effect of tetrahydroquinoline dyes structure on the performance of organic dye sensitized solar cells. Chem Mater 2007;19:4007–15.
[17] Karlsson KM, Jiang X, Eriksson SK, Gabrielsson E, Rensmo H, Hagfeldt A, et al. Phenoxazine dyes for dye-sensitized solar cells: relationship between molecular structure and electron lifetime. Chem Eur J 2011;17:6415–24.
[18] Wan ZQ, Jia CY, Duan Y, Zhou L, Zhang J, Lin Y, et al. Influence of the antennas in starburst triphenylamine based organic dye-sensitized solar cells: phenothiazine versus carbazole. RSC Adv 2012;2:4507–14.
[19] Liang M, Chen J. Arylamine organic dyes for dye-sensitized solar cells. Chem Soc Rev 2013;42:3453–88.

[20] Qu SY, Hua JL, Tian H. New D-π-A dyes for efficient dye-sensitized solar cells. Sci China Chem 2012;55(5):677–97.
[21] Zeng J, Zhang T, Zang X, Kuang DB, Meier H, Cao DR. D-A-π-A organic sensitizers containing benzothiazole moiety as additional acceptor for solar cells. Sci China Chem 2013;56(4):505–13.
[22] Tang J, Hua J, Wu W, Li J, Jin Z, Long Y, et al. New starburst sensitizer with carbazole antennas for efficient and stable dye-sensitized solar cells. Energy Environ Sci 2010;3:1736–45.
[23] Pellegrin Y, Pleux LL, Blart E, Renaud A, Chavillon B, Szuwarski N, et al. Ruthenium polypyridine complexes as sensitizers in NiO based p-type dye-sensitized solar cells: effect of the anchoring groups. J Photochem Photobiol A: Chem 2011;219:235–42.
[24] Bae E, Choi W, Park J, Shin JK, Kim SB, Lee JS. Effect of surface anchoring groups (carboxylate vs phosphonate) in ruthenium complex sensitized TiO_2 on visible light reactivity in aqueous suspensions. J Phys Chem B 2004;108:14093–101.
[25] Abbotto A, Manfredi N, Marinzi C, Angelis FD, Mosconi E, Yum JH, et al. Di-branched di-anchoring organic dyes for dye-sensitized solar cells. Eenrgy Environ Sci 2009;2:1094–101.
[26] Shang H, Luo Y, Huang X, Zhan X, Jiang K, Meng Q. The effect of anchoring group number on the performance of dye sensitized solar cells. Dyes Pigm 2010;87:249–56.
[27] Kim SJ, Heo DK, Yoo BJ, Kim B, Ko MJ, Cho MJ, et al. Two-dimensional X-shaped organic dyes bearing two anchoring groups to TiO_2 photoanode for efficient dye-sensitized solar cells. Synth Met 2012;162:2095–101.
[28] Chu HC, Sahu D, Hsu YC, Padhy H, Patra D, Lin JT, et al. Structural planarity and conjugation effects of novel symmetrical acceptor-donor-acceptor organic sensitizers on dye-sensitized solar cells. Dyes Pigm 2012;93:1488–97.
[29] Sirohi R, Kim DH, Yu SC, Lee SH. Novel di-anchoring dye for DSSC by bridging of two mono anchoring dye molecules: a conformational approach to reduce aggregation. Dyes Pigm 2012;92:1132–7.
[30] Park SS, Won YS, Choi YC, Kim JH. Molecular design of organic dyes with double electron acceptor for dye-sensitized solar cells. Energy and Fuels 2009;23:2732–6.
[31] Yang YS, Kim KD, Ryu JH, Kim KK, Park SS, Ahn KS, et al. Effect of anchoring groups in multi-anchoring organic dyes with thiophene bridge for dye-sensitized solar cells. Synth Met 2011;161:850–5.
[32] Duncan WR, Prezhdo OV. Theoratical studies of photoinduced electron transfer in dye-sensitized TiO_2. Annu Rev Phys Chem 2007;58:143–84.
[33] Yao QH, Shan L, Li FY, Yin DD, Huang CH. An expanded conjugation photosensitizer with two different adsorbing group for solar cells. New J Chem 2003;27:1277–83.
[34] Chen YS, Li C, Zeng ZH, Wang WB, Wang WS, Zhang BW. Efficient electron injection due to a special adsorbing group's combination of carboxyl and hydroxy: dye-sensitized solar cells based on new hemicyanine dyes. J Mater Chem 2005;15:1654–61.
[35] Kandavelu V, Huang HS, Jian JL, Yang TCK, Wang KL, Huang ST. Novel iminocoumarin dyes as photosensitizers for dye-sensitized solar cells. Sol Energy 2009;83:574–81.
[36] Hagfeldt A, Boschloo G, Sun LC, Kloo L, Pettersson H. Dye sensitized solar cells. Chem Rev 2010;110:6595–663.
[37] Shi J, Chai Z, Zhong C, Wu W, Hua J, Dong Y, et al. New efficient dyes containing tert-butyl in donor for dye sensitized solar cells. Dyes Pigm 2012;95:244–51.
[38] Su CY, Yu QY, Liao JY, Zhou SM, Shen Y, Liu JM, et al. Effect of hydrocarbon chain length of disubstituted triphenylamine based organic dyes on dye-sensitized solar cells. J Phys Chem C 2011;115:22002–8.
[39] Iqbal Z, Wu WQ, Kuang DB, Wang L, Meier H, Cao D. Phenothiazine-based dyes with bilateral extension of π-conjugation for efficient dye-sensitized solar cells. Dyes Pigm 2013;96:722–31.
[40] Kong XX, Kulkarni AP, Jenekhe SA. Phenothiazine based conjugated polymers: synthesis, electrochemistry and light emitting properties. Macrolmolecules 2003;36:8992–9.
[41] Wu W, Yang J, Hua J, Tang J, Zhang L, Long Y, et al. Efficient and stable dye-sensitized solar cells based on phenothiazine sensitizer with thiophene units. J Mater Chem 2010;20:1772–9.
[42] Tian H, Yang X, Cong J, Chen R, Teng C, Liu J, et al. Effect of different electron donating groups on the performance of dye-sensitized solar cells. Dye Pigm 2010;84:62–8.
[43] Wu TY, Tsao MH, Chen FC, Su SG, Chang CW, Wang HP, et al. Synthesis and characterization of three organic dyes with various donors and rhodanine ring acceptors for use in dye-sensitized solar cells. J Iran Chem Soc 2010;7:707–20.
[44] Tian H, Yang X, Chen R, Pan Y, Li L, Hagfedlt A, et al. Phenothiazine derivatives for efficient organic dye-sensitized solar cells. Chem Commun 2007:3741–3.
[45] Kim SH, Kim HW, Sakong C, Namgoong J, Park SW, Ko MJ, et al. Effect of five membered heteroaromatic linkers to the performance of phenothiazine-based dye-sensitized solar cells. Org Lett 2011;13:5784–7.
[46] Xie ZB, Midya A, Loh KP, Adams S, Blackwood DJ, Wang J, et al. Highly efficient dye-sensitized solar cells using phenothiazine derivatives organic dyes. Prog Photovolt Res Appl 2010;18:573–81.
[47] Cao D, Peng J, Hong Y, Fang X, Wang L, Meier H. Enhanced performance of the dye-sensitized solar cells with phenothiazine-based dyes containing double D–A branches. Org Lett 2011;13:610–3.
[48] Hong Y, Liao JY, Fu JL, Kuang DB, Meier H, Su CY, et al. Performance of dye sensitized solar cells based on novel sensitizers bearing asymmetric double D-π-A chains with arylamines as donors. Dyes Pigm 2012;94:481–9.
[49] Orto ED, Raimondo I, Sassella A, Abbotto A. Dye-sensitized solar cells: spectroscopic evaluation of dye loading on TiO_2. J Mater Chem 2012;22:11364–9.
[50] Tsao MH, Wu TY, Wang HP, Sun IW, Su SG, Lin YC, et al. An efficient metal-free sensitizer for dye-sensitized solar cells. Mater Lett 2011;65:583–6.
[51] Lei BX, Fang WJ, Hou YF, Liao JY, Kuang DB, Su CY. All solid state electrolytes consisting of ionic liquid and carbon black for efficient dye-sensitized solar cells. J Photochem Photobiol A 2010;216:8–14.
[52] Xu J, Zhu L, Wang L, Liu L, Bai Z. The effect of anchoring group number on molecular structures and absorption spectra of triphenylamine sensiitzers: a computational study. J Mol Model 2012;18:1767–77.
[53] Xu M, Li R, Pootrakulchote N, Shi D, Guo J, Yi Z, et al. Energy level and molecular engineering of organic D-π-A sensitizers in dye-sensitized solar cells. J Phys Chem C 2008;49:19770–6.
[54] Yang CJ, Chang YJ, Watanabe M, Hon YS, Chow TJ. Phenothiazine derivatives as organic sensitizers for highly efficient dye-sensitzed solar cells. J Mater Chem 2012;22:4040–9.
[55] Ren X, Jiang S, Cha M, Zhou G, Wang ZS. Thiophene-bridged double D-π-A dye for efficient dye-sensitized solar cell. Chem Mater 2012;24:3493–9.
[56] Ooyama Y, Nangano T, Inoue S, Imae I, Komaguchi K, Ohshita J, et al. Sensitized solar cells based on donor-π-acceptor fluorescent dyes with a pyridine ring as an elecron-withdrawing-injecting anchoring group. Chem Eur J 2011;17:14837–43.
[57] Lin H, Liu Y, Liu C, Li X, Shen H, Zhang J, et al. Effect of hydroxyl groups of coadsorbents on photovoltaic performances of dye-sensitized solar cells. J Electroanalytical Chem 2011;653:81–5.
[58] Grätzel M. Photo-electrochemical cells. Nature 2001;414:338–44.
[59] Zhang G, Bai Y, Li R, Shi D, Wenger S, Zakeeruddin SM, et al. Employ a bis-thienothiophene linkers to construct an organic chromophores for efficient and stable dye-sensitized solar cells. Energy Environ Sci 2009;2:92–5.
[60] Ito S, Zakeeruddin SM, Humphery BR, Liska P, Charvet R, Comte P, et al. High-efficiency organic dye-sensitized solar cells controlled by nanocrytalline TiO_2 electrode thickness. Adv Mater 2006;18:1202–5.
[61] Frisch MJ, Trucks GW, Schlegel HB, Scuseria GE, Robb MA, Cheeseman JR, et al. Gaussian 09. Wallingford, CT: Gaussian, Inc.; 2009.
[62] Nzaeeruddin MK, Zakeeruddin SM, Humphry BR, Jirousek M, Liska P, Vlachopoulos N, et al. Acid-base equilibria of (2,2'-bipyridyl-4,4'-dicarboxylic acid)ruthenium(II) complexes and the effect of protonation on charge-transfer sensitization of nanocrystalline titania. Inorg Chem 1999;38:6298–305.
[63] Tian H, Yang X, Cong J, Chen R, Liu J, Hao Y, et al. Tuning of phenoxazine chromophores for efficient organic dye-sensitized solar cells. Chem Commun 2009:6288–90.
[64] Tian H, Yang X, Chen R, Hagfeldt A, Sun L. A metal-free "black dye" for panchromatic dye-sensitized solar cells. Energy Environ Sci 2009;2:674–7.
[65] Yu H, Zhang S, Zhao H, Xue B, Liu P, Will G. High performance TiO_2 photoanode with an efficient electron tansport network for dye-sensitized solar cells. J Phys Chem C 2009;113:16277–82.
[66] Hara K, Dan-Oh Y, Kasada C, Ohga Y, Shinpo A, Suga S, et al. Effect of additives on the photovoltaic performance of coumarin-dye-sensitized nanocrystalline TiO_2 solar cell. Langmuir 2004;20(10):4205–10.
[67] Lu HP, Tsao CY, Yen WN, Hsieh CP, Lee CW, Yeh CY, et al. Control of dye aggregation and electron injection for highly efficient porphyrin sensitzers adsorbed on semiconductor films with varying ratios of coadsorbate. J Phys Chem C 2009;113:20990–7.
[68] Kuang DB, Uchida S, Baker RH, Zakeerudding SM, Gratze M. Organic dye-sensitized solar cells: remarkable enhancement in performance through molecular design of indoline sensitizers. Angew Chem Int Ed 2008;47:1923–7.
[69] Liao JY, Lei BX, Chen HY, Kuang DB, Su CY. Orientated hierarchical single crystalline anatase TiO_2 nanowire arrays on Ti-foil substrate for efficient flexible dye-sensitized solar cells. Energy Environ Sci 2012;5:5750–7.
[70] Tian H, Bora I, Jiang X, Garbrielsson E, Karlsson KM, Hagfeldt A, et al. Modifying organic phenoxazine dyes for efficient dye-sensitized solar cells. J Mater Chem 2011;21:12462–72.